ROYAL SOCIETY OF CHEMISTRY

PAPER

Check for updates

In situ fabrication of an anisotropic double-layer hydrogel as a bio-scaffold for repairing articular cartilage and subchondral bone injuries

Xiaotian Yu,[†ab] Zhantao Deng,[†a] Han Li,[†ab] Yuanchen Ma[a] and Qiujian Zheng ⓘ [*a]

Articular cartilage is a smooth and elastic connective tissue playing load-bearing and lubricating roles in the human body. Normal articular cartilage comprises no blood vessels, lymphatic vessels, nerves, or undifferentiated cells, so damage self-repair is very unlikely. The injuries of articular cartilage are often accompanied by damage to the subchondral bone. The subchondral bone mainly provides mechanical support for the joint, and the successful repair of articular cartilage depends on the ability of the subchondral bone to provide a suitable environment. Currently, conventional repair treatments for articular cartilage and subchondral bone defects can hardly achieve good results due to the poor self-repairing ability of the cartilage Here, we propose a bioactive injectable double-layer hydrogel to repair articular cartilage and subchondral bone. The hydrogel scaffold mimics the multilayer structure of articular cartilage and subchondral bone. Agarose was used as a common base material for the double-layer hydrogel scaffold, in which a sodium alginate (SA)/agarose layer was used for the repair of artificially produced subchondral bone defects, while a decellularized extracellular matrix (dECM)/agarose layer was used for the repair of articular cartilage defects. The double-layer hydrogel scaffold is injectable, easy to use, and can fill in the damaged area. The hydrogel scaffold is also anisotropic both chemically and structurally. Animal experiments showed that the surface of the new cartilage tissue in the double-layer hydrogel scaffold group was closest to normal articular cartilage, with a structure similar to that of hyaline cartilage and a preliminary calcified layer. Moreover, the new subchondral bone in this group exhibited many regular bone trabeculae, and the new cartilage and subchondral bone were mechanically bound without mutual intrusion and tightly integrated with the surrounding tissue. The continuous double-layer hydrogel scaffold prepared in this study mimics the multilayer structure of articular cartilage and subchondral bone and promotes the functional repair of articular cartilage and subchondral bone, favoring close integration between the newborn tissue and the original tissue.

1 Introduction

With population aging and an increased number of sports injuries, the number of people in need of joint treatments also rises. Joint injuries include not only damage to the articular cartilage but also to the subchondral bone.[1] Structurally, articular cartilage is supported by the subchondral bone, which provides an excellent mechanical environment.[2] The repair of articular cartilage injuries represents a major clinical challenge, and its unsuccessful treatment may lead to degenerative arthritis.[3] A joint has a delicate and complex structure, and most joint injuries have irregular structure (which is inconvenient for the application of the pre-constructed scaffolds).

Conventional cartilage tissue can be broadly classified into four categories: elastic cartilage, fibrocartilage, fibroelastic cartilage, and hyaline cartilage, depending on extracellular matrix (ECM) components.[4] Articular cartilage plays a significant role in the cushioning and lubrication of joints and is an essential part of the load-bearing tissue. The basic component is translucent hyaline cartilage, which has a rich ECM, especially type II collagen, and a small number of chondrocytes that secrete these ECMs.[5] Chondrocytes rely on the joint fluid for their nutrition and metabolism within the cartilage and can secrete type II collagen, polyproteoglycans, *etc.*[6] Physiologically, articular cartilage lacks blood vessels and repair-related cells, and its renewal is very slow,[7] mainly relying on the joint fluid to provide nutrients for cells to secrete and maintain the ECM and excrete metabolic waste. Therefore, the cell metabolism in articular cartilage is slow,[8] making it a non-ideal environment for the self-repair of articular cartilage defects.

The most common clinical approaches to articular cartilage repair include autologous or allogeneic cartilage grafting, the

aDepartment of Orthopedics, Guangdong Provincial People's Hospital (Guangdong Academy of Medical Sciences), Southern Medical University, Guangzhou, 510000, P.R. China. E-mail: zhengqiujian@gdph.org.cn

bGuangdong Cardiovascular Institute, Guangzhou, Guangdong, China

† These author contributed equally in the work.

microfracture of the injury site, chondrocyte injection, and arthroscopic irrigation. Although these techniques can effectively expand the treatment options for articular cartilage injuries,[9] they have many limitations: the cartilage sources required for autologous cartilage transplantation are limited; the transplantation of heterogeneous cartilage is likely to cause immune response; patients with advanced patients usually need to be replaced with artificial joints, which may lead to postoperative complications and recurrence, and the service life of artificial joints is limited. There is a high difficulty and risk of renovation surgery. Other treatments rely on the self-repair of articular cartilage. However, this does not contribute to the recovery of joint function due to the characteristics of articular cartilage and the unsuitable mechanical environment that can easily lead to the generation of fibrocartilage, which differs from articular cartilage in terms of mechanical properties and lubrication level. In recent years, the use of tissue-engineered scaffolds and corresponding seed cells for repairing articular injuries has been widely reported in the literature with the development of tissue engineering, showing good results and suggesting tissue engineering as an effective treatment method for cartilage and subchondral bone defects.[10] Cartilage tissue engineering assumes the construction of scaffold materials suitable for defect sites, the isolation of specific tissues or cells from the body, *in vitro* expansion and culturing, the inoculation of the expanded cells into a specific scaffold, and the reimplantation of the cartilage component carrying the seed cells into a defect site.[11] However, direct implantation of tissue-engineered scaffolds for articular cartilage repair can hardly achieve good results.

The subchondral bone also plays an essential role in the repair of articular cartilage. It provides mechanical support for joints and a suitable mechanical environment for articular cartilage. At the same time, most articular cartilage injuries are accompanied by subchondral bone damage, so it is difficult to obtain good repair results by repairing only articular cartilage without subchondral bone. Therefore, articular cartilage repair is tightly related to the repair of the subchondral bone[12] and should be implemented simultaneously.

A double-layer tissue engineering scaffold is promising for repairing cartilage and subchondral bone damage. The double-layer scaffold can repair both articular cartilage and subchondral bone, and the repair of the subchondral bone can provide an excellent mechanical environment for articular cartilage regeneration.

The use of agarose to construct double-layer scaffolds for repairing articular cartilage and subchondral bone has been reported in the literature.[13] However, the reported double-layer scaffolds were mainly connected by adhesion between the double-layer materials or *via* physical bonding, resulting in a poor mechanical connection between the double-layer scaffolds. The lack of consistency between the selected double-layer scaffold materials resulted in poor continuity between the double-layer scaffolds, and the repair failed due to the easy dislodgement of the double-layer materials under *in vivo* stress. Therefore, promoting the connection between the multilayer hydrogels is one of the challenges in constructing tissue engineering scaffolds

for articular cartilage repair. In addition, to address the specific irregularity of joint defect sites, many tissue-engineered scaffolds for cartilage defect repair were constructed using 3D printing.[14] However, most of these scaffolds were fabricated *in vitro*. At the same time, a joint represents a complex and narrow space, so transplanting the prepared scaffold material into the defect site is an issue that must be considered in applying scaffold materials. Grafting a large volume of the preformed scaffold into the injury site can easily lead to secondary injury. Furthermore, the joint cavity must inevitably be opened when implanting the engineered scaffold into the articular cartilage defect site, also causing a secondary injury. Therefore, in situ-moldable bioprosthetics based on injectable hydrogel scaffold materials are favorable in terms of material fitting to the wound and avoiding secondary injury during grafting. An injectable hydrogel scaffold can be easily implanted into a defective area and reach the trauma surface only by syringe injection. At the same time, the hydrogel can fill in the trauma surface after injection, which is very suitable for the narrow and complicated areas of articular cartilage and subchondral bone defects. A successful design can effectively prevent repair failure and contribute to avoiding secondary surgery.

Scaffold materials for tissue engineering must have specific properties, such as good mechanical properties, high porosity, moderate swelling properties, and good biocompatibility,[15] providing a suitable growth environment for seed cells inside the scaffold. The high porosity and good swelling properties ensure that cells inside the scaffold material can transport nutrients and discharge waste from the external environment, while good biocompatibility ensures the absence of adverse cytotoxic reactions inside the scaffold and the body.[16] For double-layer scaffolds for articular cartilage and subchondral bone repair, the degree of bonding between the two layers is also essential because they are under constant stress, *e.g.*, the bonding should be strong enough to prevent the material from separating under stress, thus affecting the repair. From the literature, we found that the hydrogel composed of agarose and sodium alginate is hydrophilic and porous, which is suitable for cell growth and metabolic waste removal.

Seed cells play an important role in tissue engineering as one of the three main elements. Due to the natural configuration of articular cartilage, its weak bioactivity, and the lack of blood vessels and repair-related cells, articular cartilage renews slowly, making the repair of even minor defects very difficult.[17] Therefore, seed cells are critical for articular cartilage repair. In articular cartilage repair, chondrocytes play an essential role, and they can secrete a large amount of cartilage matrix, especially collagen II, which contributes to articular cartilage repair.[18] However, in practice, tissue engineering scaffolds need to carry many seed cells for tissue repair. The source of articular chondrocytes is minimal, and the threshold for using only articular chondrocytes as the seed cell technology for articular cartilage repair is high. It was also reported that articular chondrocytes undergo dedifferentiation in the process of proliferation, making it challenging to maintain their chondrocyte phenotype in the long term, and as chondrocytes proliferate *in vitro*, their cartilage-related gene expression and

the secretion of ECM reduce.[19,20] Bone marrow MSCs are also present in joints and play a role in cartilage repair. They are abundant and expand easily, and they have been used as typical tissue engineering seed cells for bone tissue repair.[21,22] However, bone marrow MSCs only differentiate into chondrocytes under many chondrogenic conditions. Such induced differentiation tends to lead to hypertrophy and calcification of cartilage, which may result in endochondral osteogenesis.[23]

According to the literature, the co-culturing of bone marrow MSCs with chondrocytes is an effective way to overcome the limited number of chondrocytes and their tendency to de-differentiate; the problems of cartilage hypertrophy and endochondral osteogenesis caused by using only bone marrow MSCs can also be alleviated, contributing to the formation of hyaline cartilage.[24,25] In this co-cultured system, the seeded chondrocytes can induce differentiation of bone marrow MSCs to chondrocytes through intercellular communication, thus reducing the required amount of chondrocytes as seed cells; on the other hand, TGF-β and BMP-2 secreted by bone marrow MSCs can up-regulate the production of cartilage matrix, nourishing chondrocytes to some extent and maintaining their chondrocyte phenotype,[24] reducing chondrocyte dedifferentiation and even enabling dedifferentiated chondrocytes to redifferentiate by co-culturing with bone marrow MSCs. Using this chondrocyte-bone marrow MSCs co-culture system reduces the number of chondrocytes and largely overcomes the problem of insufficient chondrocyte source; it also nourishes the chondrocytes with bone marrow MSCs, allowing the chondrocytes to preserve their phenotype to a large extent.

In a previous study,[26] we reported an in situ-formed bioscaffold based on dECM, which possessed anisotropy and mimicked the multilayered structure of cartilage. However, the physical strength of the decellularized matrix was low, so we propose a novel bio-scaffold that uses agarose as a continuous phase, a decellularized matrix as a cartilage repair layer, and Ca^{2+} cross-linked sodium alginate as a bone repair layer. This novel scaffold exhibits high mechanical strength, suitable porosity, and good bioactivity. It is able to gel near the body temperature, while the chondrogenic repair layer and osteogenic repair layer material has a common base material, making a tight bond between the two layers. At the same time, the co-culture system of chondrocytes and bone marrow MSCs can reduce the demand for chondrocytes and promote better articular cartilage repair.

2 Experimental part

2.1 Preparation of decellularized extracellular matrix

The preparation and characterization of dECM is similar to the method we reported before.[26] Briefly, cartilage tissue was cut into 1 mm thick slices, frozen with liquid nitrogen and grounded into a coarse powder. 1 g of tissue powder was dispersed in 500 mL 1% SDS/PBS solution and stirred for 72 h. The SDS solution was replaced every 24 h. The samples were transferred into 500 mL 0.1% EDTA/PBS solution for 24 h and dialysis with deionized water to remove residual chemicals. Finally, the resulting dECM was frozen dried and ground into a fine powder and stored at −20 °C for future usage.

2.2 Characterization of decellularized extracellular matrix

Prepared dECM was further digested using a HCl (0.01 M) solution of pepsin (1 mg mL^{-1}), for a typical procedure, 1 g of dECM was dispersed in 100 mL pepsin solution, and the residual was subsequently removed by a centrifuge. The upper-layer solution was centrifuged for 30 min at 10 000g in a phenol/chloroform/isovalyl alcohol (25 : 24 : 1) mixed solvent. Dialysis was used to extract the water layer in the obtained sample. DNA and precipitation were performed using a 3 M solution of sodium acetate/ethanol (v/v = 1 : 20) overnight at −20 °C. The extracted DNA samples were dehydrated at room temperature in a vacuum oven and dissolved using TE buffer. Finally, the PicoGreen fluorescent dye and the Modulus detector were used to determine the content of the residual DNA.

The hydroxyproline detection kit produced by Sigma was used to measure the collagen content and was calculated by the amount of hydroxyproline. The dECM and untreated cartilage tissue was hydrolyzed using 6 M HCl at 120 °C of water for 3 h and cooled to 65 °C. Subsequently, 100 L of chloramine T concentrate and oxidation buffer mixed solvent was added to the sample and incubated at room temperature for 5 min. An additional 100 L of dimethylbenzaldehyde solution was added to each sample and then incubated for 90 min at 60 °C. An Infinite M200 multifunctional microplate reader was used to read the absorbance at 560 nm and draw standard curves.

Glycosaminoglycan content was measured using an amino-glycan sulfate assay kit from Biocolor, and dECM was digested with untreated cartilage tissue in 0.01 M HCl using pepsin (1 mg mL^{-1}). A 0.01 M HCl solution of pepsin was used as a control during testing.

The amount of antigen residue in the DECM is calculated with a (α-GAL) Activity Assay Kit, 1 mL of Extract solution is added in to the DECM to 0.1 g of tissue, and fully homogenized on ice bath. Centrifuge at 15 000 rpm for 20 minutes at 4 °C to remove insoluble materials, and take the supernatant on ice before testing. The standard curve was established with A_{400nm} of the standard solution of 200, 100, 50, 25, 12.5, 6.25, 0 nmol mL^{-1} with distilled water. The lysed samples and standard curve samples are mixed with equal volumes of anti-α-Gal antibodies respectively. After reacting standing and centrifuging, the appropriate supernatant was taken and react it with the solid-phase antigen. The residual anti-α-Gal antibodies in the samples are analyzed according to the ELISA method.

Enment was performed using OCT embedding at −20 °C and subsequently cut into 7 m thick sections for hematoxylin/eosin staining. A fluorescence inverted microscope was used to observe the staining results.

2.3 Preparation of the double-layer hydrogel scaffold

2.3.1 The preparation of the sterile 2% sodium alginate solution. A sterile 2% sodium alginate solution was prepared by sterilizing a 100 mL flask and an accompanying magnetic stirring rotor in an autoclave, the flask was sterilized on an ultra-clean table for 30 min. 2 g of sodium alginate powder was dispersed with 100 mL of deionized water in the sterilized flask, and transferred to the ultra-clean table for 30 min. The flask was

sealed with a sealing film, and placed on a magnetic stirrer to stir for 2–4 h. A sterile 2% sodium alginate solution was obtained when the sodium alginate powder was completely dissolved. The sodium alginate solution should be stored in a refrigerator at 4 °C and protected from light.

2.3.2 The preparation of the sterile 2% agarose solution. 2 g of agarose powder was weighed and transferred to an ultra-clean table using UV sterilization for 30 min; then, 100 mL of autoclaved deionized water was heated to boiling. 2 g of sterilized agarose powder was added into boiling deionized water and kept boiling for 30 s to obtain a 2% sterile agarose solution, which could be retained in the liquid state above 50 °C. After solidification, the solid was reheated to boiling to regain the liquid agarose solution.

2.3.3 The preparation of SA/agarose injectable hydrogels. After the sterile 2% sodium alginate solution and the 2% agarose solution in the liquid state were prepared as described above. 2.5 mL of each solution are drawn into two syringes respectively, the SA solution was first injected into the mold and agarose containing Ca^{2+} (2%, w/v) was injected into the SA solution. As the temperature of the mixed solution decreased, the agarose started to gel slowly, yielding an injectable SA/agarose hydrogel. The injectable hydrogel prepared with the above SA/agarose ratio exhibited a gelling temperature of about 37 °C.

2.3.4 The preparation of dECM/agarose injectable hydrogels. After the sterile 2% dECM solution and the 2% agarose solution in the liquid state were prepared as described above. 2.5 mL of each solution are drawn into two syringes respectively, the dECM solution was first injected into the mold and agarose was injected into the SA solution. As the temperature of the mixed solution decreased, the agarose started to gel slowly, yielding an injectable dECM/agarose hydrogel. The injectable hydrogel with the above dECM/agarose ratio exhibited a gelling temperature of approximately 37 °C at room temperature.

2.3.5 The preparation of dECM/SA/agarose injectable hydrogels. Sterile 2% sodium alginate solution prepared as described above was mixed with the 2% agarose solution in the liquid state. 2.5 mL of the SA solution was drawn into one syringe, and 2.5 mL of the dECM/agarose solution was drawn into the other syringe. The two solutions were injected successively into the mold. As the temperature of the mixed solution decreased, the agarose started to gel slowly, resulting in an injectable dECM/SA/agarose hydrogel. The injectable hydrogel prepared with the above dECM/SA/agarose ratio exhibited a gel temperature of approximately 37 °C at room temperature.

2.4 Morphological characterization of the double-layer hydrogel scaffold

The gelated double-layer hydrogel scaffold was removed from the mold, and the joint part of the double-layer hydrogel scaffold was selected and sliced to a suitable thickness with a scalpel and placed on a slide to observe its morphology under a light microscope. At the same time, the double-layer hydrogel was frozen at −80 °C for 30 min, then transferred to a pre-cooled freeze-dryer and freeze-dried under a vacuum for 12 h. Ice crystals inside the

hydrogel sublimated to obtain the lyophilized hydrogel scaffold. The lyophilized hydrogels were cut into thin slices with a scalpel and fixed on holders. After gold sputtering with an ion sputter, the material was placed in a scanning electron microscope (SEM, Hitachi S-4800) to observe the clear porous structure, especially the hollow structure of the double layer and the connection between the two layers.

2.5 Characterization of the mechanical properties of the double-layer hydrogel scaffold

2.5.1 The characterization of swelling ratio. SA/agarose hydrogels, dECM/agarose hydrogels, and double-layer hydrogels were prepared as described above and placed in a freezer at −80 °C for 30 min and then dried in a freeze-dryer. The lyophilized hydrogels were obtained after 12 h of freeze-drying. After the water in the scaffold was sublimated, the weight of the lyophilized hydrogel was measured on an electronic balance. An appropriate amount of deionized water was added to immerse the hydrogel, and the hydrogel was removed from the deionized water at 20, 40, 60, 80, 100, 120, and 180 min; the surface of the hydrogel was wiped with filter paper to remove deionized water, and the weight of the hydrogel was measured again.

2.5.2 The characterization of mechanical properties. As described above, SA/agarose hydrogels, DECM/agarose hydrogels, and double-layer hydrogels were prepared. The hydrogels were injected into cylindrical molds made of polytetrafluoroethylene with a height of 1 cm and a radius of 1 cm. Then, the hydrogels were removed after gelling to maintain their moist states. The mechanical properties were tested using a universal testing machine as follows:

After gelation, the hydrogel was placed on the test platform and kept in its wet state; the compression speed was set to 0.1 mm min; when the test end touched the upper plane of the hydrogel, the force on the test end started to be recorded; as the compression kept increasing, the hydrogel was continually compressed, the force kept increasing and finally ruptured; at this time point, the force on the test end changed significantly, so the material rupture could be detected. The stress magnitude on the hydrogel at rupture was recorded, and the double-layer material rupture was photographed simultaneously. The stress–strain curves of material deformation were recorded, and the modulus of elasticity of the material was calculated from the linear part of the stress–strain curve.

2.5.3 The characterization of swelling ratio. The anisotropic hydrogel was fabricated into a cylinder with a diameter of 5 mm and a length of 10 mm. After weighed, the cylinder was placed in massive volume of water for the observation of natural degradation. The mass of the anisotropic hydrogel was measured every 2 days. Then the hydrogel was dried by filter paper, weighed and calculated the percentage of total weight.

2.6 *In vitro* cell toxicity and proliferation

Bone marrow mesenchymal stem cells (Rt-BMSCs) were bought from Procell Life Science & Technology Co., Ltd (Wuhan, China). The cells were cultured in a complete medium containing Dulbecco's modified Eagle's medium (DMEM, Gibco) with 10% fetal

bovine serum (FBS) and 1% penicillin/streptomycin (P/S). The cells were cultured in a constant-temperature cell chamber at 37 °C with 5% CO_2, and the medium was changed every 24 h using a freshly pre-warmed medium.

The freezing tube is put into a 37 °C water bath to melt quickly. After drying and disinfecting, continue operation in a clean workbench. The cell suspension is aspirated into the centrifuge tube, then the amount of cell suspension culture medium and mixed. The mixture is centrifuged at 1000 rpm min^{-1} for 3–5 min. The upper liquid is discarded, and appropriate amount of culture medium is added to re-disperse the cells. The cell suspension is inoculated into one or more culture bottles at a suitable density, replenish the culture medium, shake well, and placed in an incubator for culture. The cell morphology and growth status were observed under an inverted microscope on day 2. The cells can be passaged, when the cell growth density reaches 80% to 90%. The culture medium is aspirated. After washing with PBS for 1–2 times. An appropriate amount of trypsin containing EDTA was added into the bottle according to the size of the culture bottle to cover the entire bottom of the culture bottle. Put the culture bottle into a 37 °C CO_2 incubator for digestion. After 2 to 5 minutes, the bottle was taken out and observed under an inverted microscope. When 70% to 80% of the cells have shrunk and become rounded, the bottle is tapped gently again to make the remaining cells peels off the culture bottle, and then immediately add twice the amount of trypsin culture solution to stop digestion. Aspirate all the cell suspension into the centrifuge tube and centrifuge at 100 rpm min^{-1} for 3–5 min. Discard the supernatant, add appropriate amount of culture medium to resuspend the cells, and mix gently to evenly disperse the cells. An appropriate amount of cell suspension is inoculated into a new culture bottle at a suitable density, replenish the culture medium, shake well, and place it in a 37 °C CO_2 incubator for culture. Repeat the above process to select cells for subsequent experiments. Only young cells from the 3rd to 7th generation were used in this experiment.

The resulting hydrogel loaded with MSCs was added to the corresponding cell culture medium for continued culture, which was changed every two days. After incubation for 20 days, CCK 8 staining was performed to assess cell survival in the DECM hydrogel. A mixture of CCK-8 solution and culture medium (1 : 9, v/v) was added to the wells of each group. Optical density values of the supernatants were determined after incubation for 2 h using a spectrophotometric microplate reader at 450 nm. The numbers of viable and dead cells in the results were calculated separately, and cell viability was obtained as the number of viable cells/total cell number in the treatment.

2.7 qT-PCR

To determine the induction of osteogenic differentiation of bone marrow MSCs in SA/agarose hydrogels and the chondrogenic differentiation of bone marrow MSCs in dECM/agarose hydrogels. A real-time fluorescence quantitative polymerase chain reaction (Realtime-PCR) is applied to quantify the expression of corresponding genes in bone marrow MSCs.

2.8 Animal experiments

These experiments were approved by the Animal Management Committee of Guangdong Provincial People's Hospital. 32 female SD rats weighing 350–410 g at 6–8 weeks were selected and randomly divided into 4 groups, labeled as A, B, C, and D, respectively. The weight of each rat was weighed and recorded. A dilute pentobarbital solution with physiological saline as 1% injectable liquid was injected intraperitoneally at a 40 mg kg^{-1} dose according to the rat's body weight. We searched for blood after the syringe entered the abdominal cavity and drew back to prevent the syringe from sticking into the organs. The rats were anesthetized, placed in a cage, and closely observed for breathing. After the completion of anesthesia, the sterile surgical towel was spread. The selected rat was fixed in the right-side position, the hair was removed from the hind limbs of the rat using a hair removal device, and the skin was disinfected with iodophor and alcohol after hair removal. The surgical area was also disinfected with iodophor. A longitudinal incision was made at the joint of the rat's hind limb, and the subcutaneous tissue and joint capsule of the rat's hind limb were incised separately, layer by layer. By dislocating the patella of the rat, the femoral trochlea was exposed. A cartilage and subchondral bone defect with a depth of 1 mm was drilled out of the femoral trochlea with a 0.8 mm radius grinder, controlling the depth slightly above the thickness of the articular cartilage to construct a model of the articular cartilage and subchondral bone defect. During the grinding process, the grinding site should be cooled down with saline at regular intervals. At the same time, to prevent the interference of other irrelevant factors, the penetration of the bone marrow cavity and the leakage of bone marrow blood from the basal should be avoided. The above model of articular cartilage and subchondral bone defects in rats was constructed. After constructing the defect models of articular cartilage and subchondral bone, the defect areas were flushed with saline to aspirate cartilage debris, *etc.* Group A was set as a black group, and Groups B and C were injected with SA/agarose and dECM/agarose hydrogels. Group D was injected with a double-layer hydrogel scaffold, and the amount of each scaffold injected in Group D should be carefully combined with the specific cartilage and the ratio of subchondral bone. After injection of the brace gel, the dislocated patella was repositioned, and the joint was moved to see whether the gel was set entirely and did not detach. The medial support band and the subcutaneous and skin tissues were also closed and reinforced with absorbable sutures. Postoperatively, the rats were injected with penicillin according to their body weight to prevent infection. The knee joints of the experimental rats were not fixed after surgery. The wound site sutures were observed, the stitches were replaced in case some sutures fell off, and the wounds were disinfected with iodophor daily to prevent infection.

2.9 Histological staining

At weeks 4 and 8 after implantation of the injectable hydrogel, four rats in each group were euthanized with an overdose of 1% pentobarbital solution. The rats were subjected to routine

necropsy to observe whether the hydrogel injected into the rats had any adverse effects, mainly to observe any obvious accumulation of fluids and edema in the joint cavity of the rats injected with the tissue-engineered scaffold. After confirmation, the joint parts of the rats were immersed and fixed in a 10% formalin buffer. The articular cartilage and subchondral bone were left after the removal of the surface attachments. The appearance of the articular cartilage was photographed using a digital camera to observe the repair of the articular cartilage defects to record the grouping as an external image.

Articular cartilage was stored in the formalin solution and decalcified using an EDTA decalcification solution. Sections were followed by hematoxylin-eosin, safranine O-fast green, and collagen II immunohistochemical staining and observed using an inverted fluorescence microscope to evaluate the repair process.

2.10 Statistical analysis

All quantitative data are verified by analysis of variance using one way ANOVA Fixed Effects Model in SPSS 26. Experiment data with P values of less than 0.005 were considered statistically significant. Error bars in all figures represent standard error.

3 Results and discussion

The results showed that the content of double-stranded DNA decreased from 110.5 ng mg^{-1} to 10.79 ng mg^{-1} by physical, chemical, and of collagen increased from 41.97% to 73.51%, the content of glycosaminoglycan decreased from 18.76% to 5.808%, and the clearance efficiency of α-GAL is 96.42% (Fig. 1). The original chemical components are basically maintained, and the decrease in glycosaminoglycan content may be caused by using SDS, which will be adjusted by adding the corresponding raw materials in the subsequent preparation process. After embedding the cartilage tissue and acellular cartilage tissue, HE staining found that the purple nucleus disappeared in the cartilage tissue after decellularization, which proved the degree of decellularization (Fig. 2).

Three types of hydrogels, SA/agarose, dECM/agarose, and SA/dECM/agarose were freeze-dried and then sampled for SEM examination. dECM/agarose and SA/agarose hydrogels exhibit isotropic structures with a uniform internal cavity size of 12 and 8 μm, respectively (Fig. 2a and b). The double-layer anisotropic hydrogel structures were fabricated by controlled diffusion, where two phases of different densities were mixed; the mixed pre-gel solution underwent phase separation due to buoyancy (caused by density differences), producing an anisotropic structure. To preserve this structure, the solution was placed at 37 °C, and after 10 min of curing, the gelation process was completed, and the anisotropic hydrogel was obtained. The final morphology and structure of the hydrogel were created by adjusting the viscosity and density of the pre-gel solution.

Anisotropic hydrogels were frozen immediately after synthesis to reduce the effect of sample preparation on morphological characterization. Direct *in situ* observation of the internal structure using cryogenic SEM also confirms the directional distribution of pore sizes at different locations (Fig. 2c and d).

Fig. 3 shows the modulus of elasticity and swelling ratio of the SA/agarose, dECM/agarose, and double-layer hydrogels. Fig. 3a shows the storage modulus of the three materials, where the hydrogels undergo significant deformation under increasing forces. The SA/agarose hydrogel can withstand higher forces and exhibits better elastic deformation. The storage modulus of SA/agarose hydrogel is 20.83 kPa. The storage modulus of dECM/agarose hydrogel is 5.10 kPa, which compromise the mechanic property of the entire hydrogel, leading to a storage modulus of 14.8 kPa, barely achieve the minimum mechanic property of original cartilage.[27,28] Fig. 3b shows the swelling ratio of the three hydrogels. The swelling curve of the lyophilized double-layer hydrogel scaffold material indicates that the swelling ratio is approximately stable after soaking in deionized water for 100–120 min, without noticeable changes in the material swelling after 120 min. The swelling performance of the SA/agarose hydrogel is the highest among the three hydrogels, reaching about 20 ± 2 times in 120 min, while the swelling of the dECM/agarose hydrogel is about 11 ± 1 at the same time. The swelling performance of the double-layer material was in between the previous two hydrogels, *i.e.*, about 15 ± 1 times. All three materials exhibit good swelling properties. The porosity in the lyophilized double-layer hydrogel scaffold material is $70.95 \pm 1.62\%$ in the SA/agarose hydrogel and $64 \pm 1.83\%$ in the lyophilized dECM/agarose hydrogel as measured by ethanol immersion method. The good porosity of both hydrogel scaffold proved that the materials have good porosity suitable for use as scaffold materials for tissue engineering. The degradation efficiency of the anisotropic hydrogel were further tested, and the results showed that the weight of hydrogel decreased gradually with time, and the hydrogel was almost degraded on the 18th day (Fig. 3c).

The proliferation level of the cells was monitored to characterize the biocompatibility of these hydrogels using CCK8 test kits. The samples were taken every two days for 20 days (Fig. 4).

The expression of osteogenic-related genes in bone marrow MSCs co-cultured with SA/agarose hydrogels carrying bone marrow MSCs at different co-culture times is shown in Fig. 5a and b. The bone marrow MSCs were co-cultured with the SA/agarose hydrogel carrying bone marrow MSCs for 7, 14, and 21 days. The expression of osteogenesis-related genes ALP and collagen I in bone marrow MSCs was measured. The expression of ALP and collagen I is significantly up-regulated after 21 days of co-culturing, and the ALP gene is 2.38-fold higher than that after 7 days of co-culturing; the gene of collagen I after 21 days of co-culturing is 2.78-fold higher than that of after 7 days of co-culturing. This indicates that the co-culturing of bone marrow MSCs and the SA/agarose hydrogel can significantly promote the osteogenic differentiation of bone marrow MSCs. The expression of genes associated with chondrogenic differentiation after co-culturing bone marrow MSCs with dECM/agarose hydrogels carrying chondrocytes and bone marrow MSCs is shown in Fig. 5c and d. The expression of collagen II and Acan genes was significantly up-regulated after 7 days of co-culturing
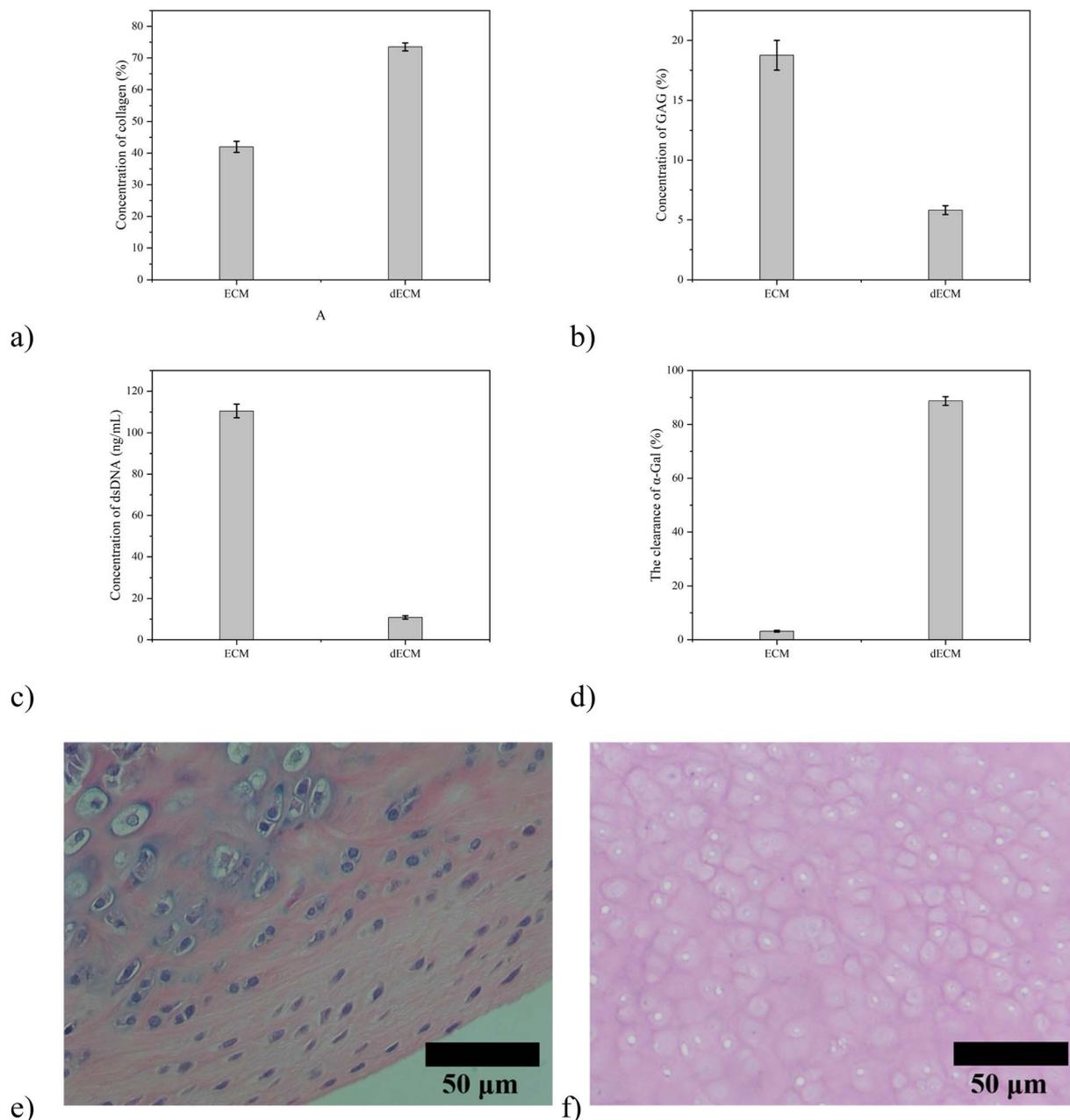
Fig. 1 Changes in the content of various components before and after decellularization of cartilage tissue: (a) collagen; (b) GAG; (c) dsDNA; (d) α-Gal. The HE staining images of (e) normal cartilage tissue; (f) dECM.

of bone marrow MSCs and hydrogels carrying chondrocytes and bone marrow MSCs. After another 14 days of co-culturing, the expression of the collagen II gene is 2.33-fold, and the Acan gene is 1.718-fold higher than after the first week. This indicates that the chondrogenic differentiation of bone marrow MSCs can be induced by co-culturing with dECM/agarose hydrogels carrying chondrocytes and bone marrow MSCs.

In animal experiments, all rats were fully awakened after surgery with no significant adverse effects. There was no significant postoperative septicemia or infection, swelling, or deformity of the hind limb joints that would warrant the exclusion of samples. The rats were euthanized at weeks 4 and 8

postoperatively with an anesthetic overdose, and the joints were removed without significant hyperplasia or inflammation (Fig. 6).

The first row shows the appearance of the articular cartilage 4 weeks after surgery, and the red circle shows the new articular cartilage. In terms of the visual effect, the group injected with the double-layer material (the SA/agarose hydrogel with bone marrow MSCs and the dECM/agarose hydrogel with chondrocytes and bone marrow MSCs) and the group injected only with the cartilage layer (the dECM/agarose hydrogel with chondrocytes and bone marrow MSCs) exhibits more new articular cartilage and a smoother surface at the defect site. The
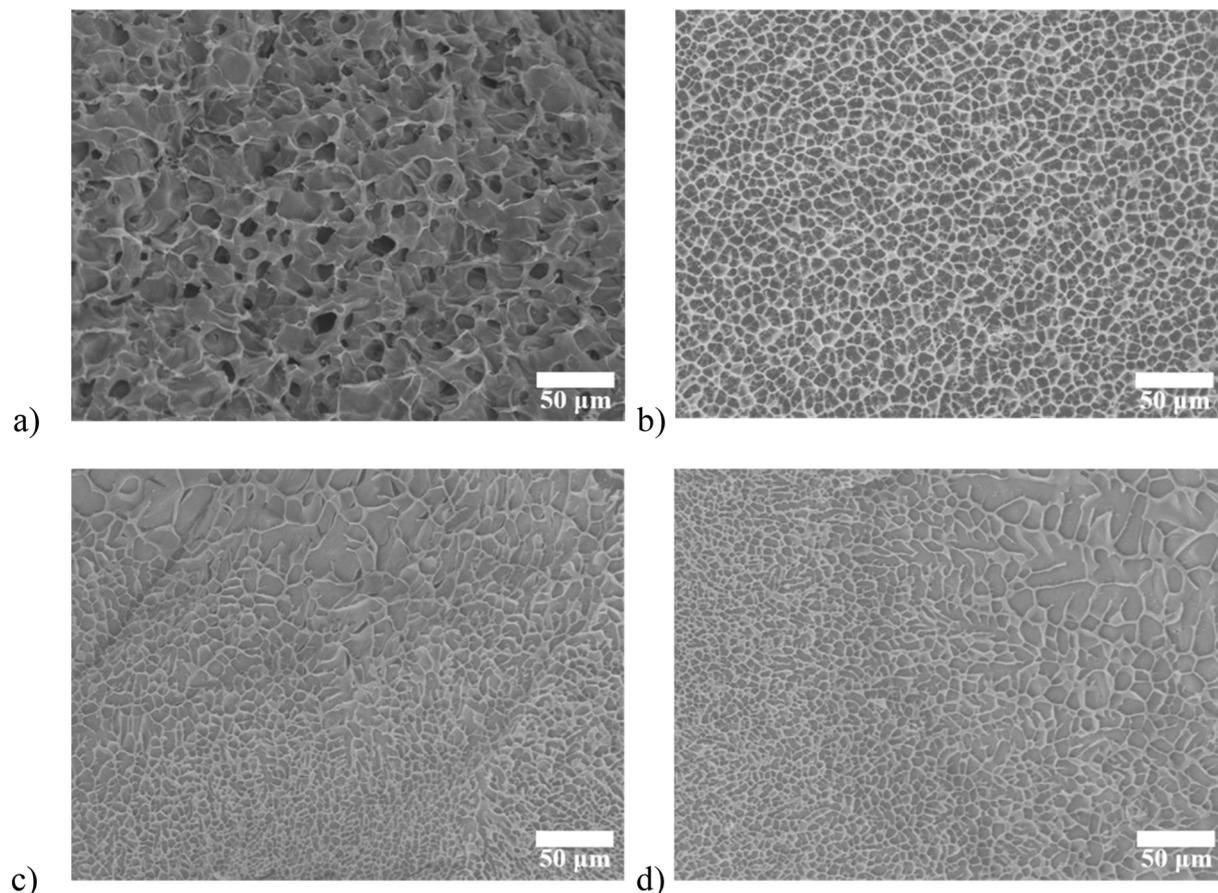
Fig. 2 SEM images of (a) SA/agarose hydrogel; (b) DECM/agarose hydrogel. cryogenic SEM images of (c) double-layer hydrogel (longitudinal cutting); (d) double-layer hydrogel (cross-sectional cutting).

defect site is well-filled, and the new tissue is better integrated with the surrounding original tissue. The new tissue is more closely integrated with the surrounding tissue. In contrast, the defect site injected with the osteogenic layer material (the SA/agarose hydrogel carrying bone marrow mesenchymal stem cells) exhibits more new cartilage than the blank control group but significantly less than the group injected with the double-layer material and the group injected with chondrogenic layer material; at the defect site injected with the osteogenic layer material, the new cartilage surface is rougher and has more significant gaps and a low degree of binding with the surrounding tissue.

The second row shows the appearance of the articular cartilage defects 8 weeks after surgery. The defects are repaired to varying degrees in different groups. In the blank control group, there is partial cartilage repair, but the approximate contours of the defect edges can still be faintly observed. In contrast to the results after 4 weeks, the cartilage regeneration is significantly better in the defect area injected with the double-layer repair material than in the other three groups that included the cartilage layer repair material; the new tissue has a glossy surface and is tightly integrated with the surrounding tissue, and the articular cartilage defect is largely filled. In contrast, the group with the injected cartilage layer material

exhibits more obvious growth of new cartilage at the defect site. However, the surface finish is not as good as the new cartilage at the defect site with the injected double-layer hydrogel scaffold, and the bonding degree to the surrounding tissues is lower than that of the group with the injected double-layer material.

In contrast, the group injected only with the osteogenic layer material exhibits more cartilage neoplasia and better integration with the surrounding tissues. The above cartilage repair appearance maps at different time points tentatively illustrate that the double-layer consisting of SA/agarose carrying bone marrow MSCs and dECM/agarose carrying chondrocytes and bone marrow MSCs can promote the regeneration of articular cartilage, and the new articular cartilage tissue is tightly bound to the surrounding tissue. Also, comparing the group injected with a single layer of material and the group injected with a double layer of material, the short-time cartilage repair was good in the former, while in terms of long-time cartilage repair, the group injected with the osteogenic layer material only exhibits a comparable or even better repair effect than the group injected with the cartilage layer material. This may infer that by the dECM/agarose carrying chondrocytes and bone marrow MSCs. The direct repair of the cartilage layer by agarose hydrogels carrying chondrocytes and bone marrow MSCs can be effective in a short time; however, without the excellent support
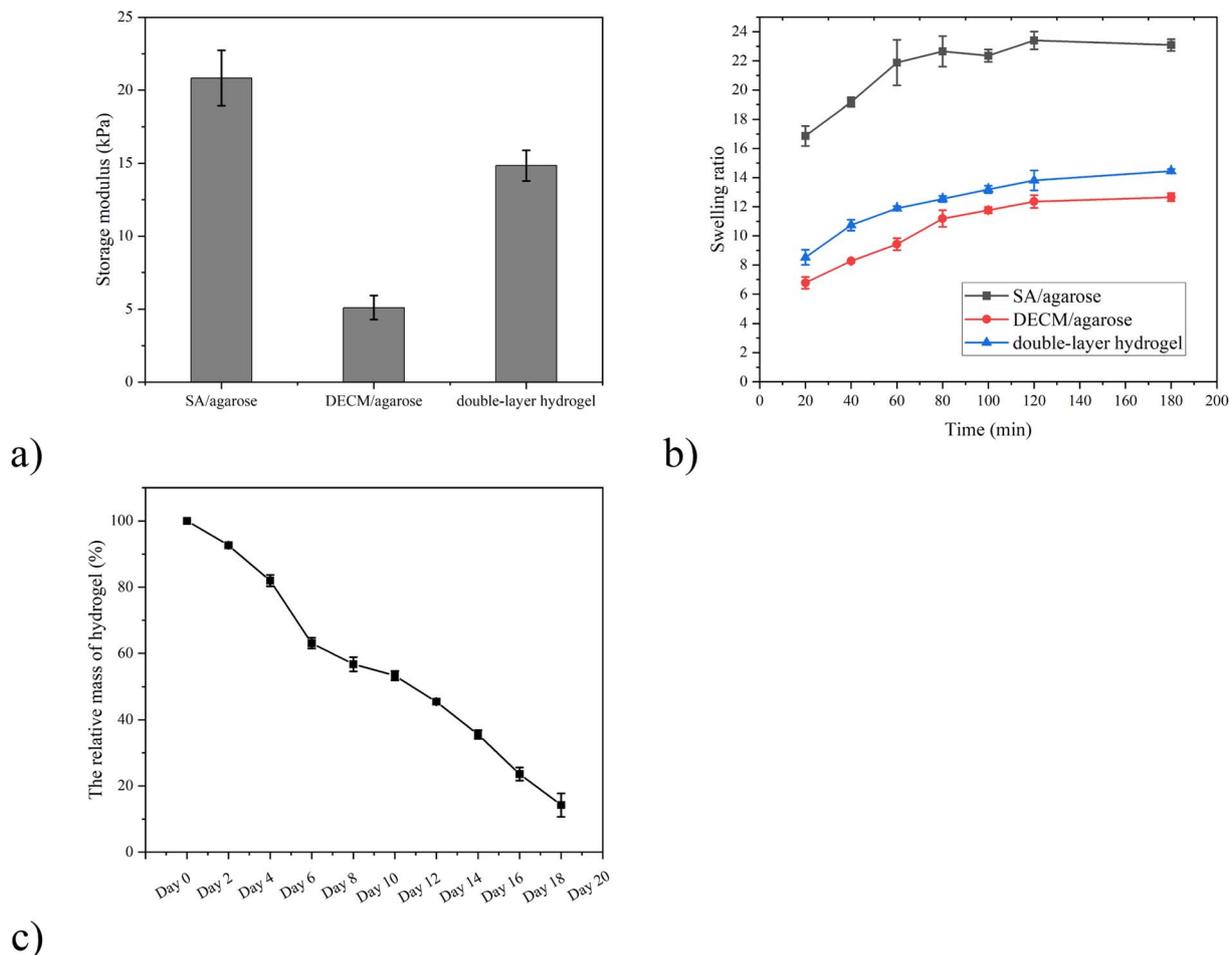
Fig. 3 (a) Storage modulus and (b) swelling ratio of three as-synthesized hydrogels. (c) The biodegradation efficiency of SA/agarose/dECM hydrogel.

and mechanical environment provided by the subchondral bone, even if the repair of the cartilage layer is carried out, the repair effect cannot be preserved for a longer time. This agrees with the literature findings that the mechanical environment provided by the subchondral bone is important for articular cartilage regeneration and maintaining normal morphology.

Fig. 7 show the results of the HE staining of paraffin sections after the new tissue was taken and decalcified at weeks 4 and 8, respectively. Compared to the previous tests, normal articular cartilage and subchondral bone were added as positive controls to better demonstrate and compare the repair, especially the articular cartilage morphology (Fig. 7). The HE staining of the repaired tissue at the defect site injected only with the osteogenic scaffold (the 1st column) shows a good repair of the subchondral bone; however, the penetration of bone tissue from the subchondral bone into the articular cartilage appears, the demarcation line between the articular cartilage and the subchondral bone is not obvious, and the subchondral bone shows slight bone tissue hyperplasia, the distribution of chondrocytes in the articular cartilage is irregular, and the edges of the articular cartilage are not smooth and appear more concave, with more depressions. The new cartilage is not tightly integrated with the original tissue, and the new cartilage layer is thin. There is some general articular cartilage and subchondral bone repair, especially subchondral bone. However, the repaired articular cartilage is poor, and the subchondral bone is excessively repaired. In the group injected with the cartilage layer scaffold only (the 2nd column), the new cartilage tissue exhibits the thickness in several groups, even slightly exceeding the thickness of the normal cartilage tissue in the joint. However, many chondrocytes are irregularly distributed in the newly formed cartilage. Also, many chondrocytes are not in the cavity, the new cartilage tissue staining color is not uniform, and there might be some unevenness in the new cartilage tissue. The ECM composition and density are inconsistent. The cartilage tissue grows into the subchondral bone, and the boundary between the new cartilage and the subchondral bone is blurred; the repair effect in the underlying bone tissue is only average, with a few bone trabeculae and irregular shape; in general, the sole injection of the cartilage layer material in the articular cartilage and subchondral bone defects may lead to excessive cartilage proliferation, hindering the effective repair of the subchondral bone. In contrast, defects injected with the double-layer material exhibit a moderate cartilage thickness,
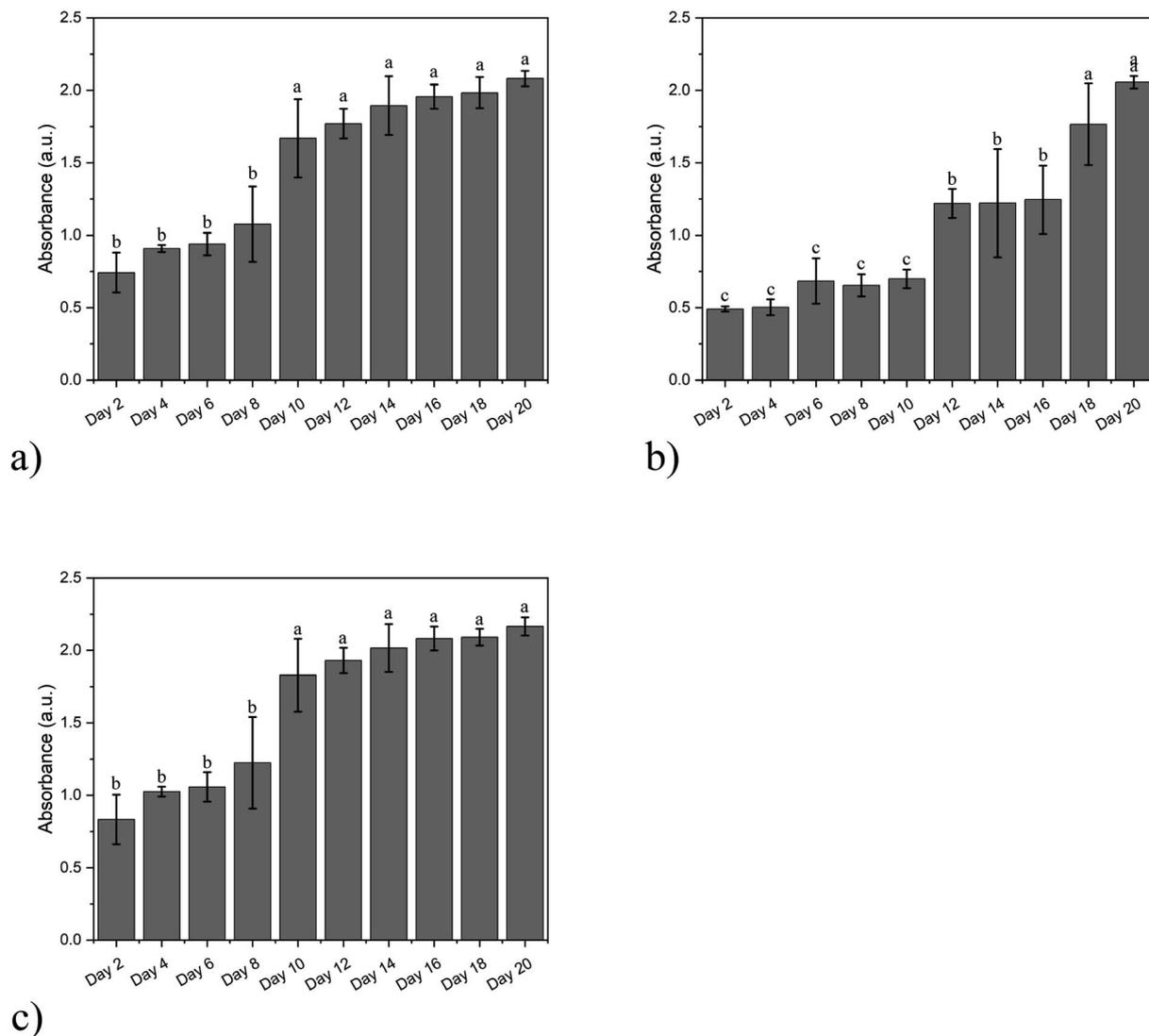
Fig. 4   The proliferation level of cells cultured in (a) SA/agarose hydrogel, (b) dECM/agarose hydrogel, and (c) double-layer hydrogel.

the smooth surface of new cartilage, and a relatively regular distribution of chondrocytes within the cartilage, with chondrocytes in the cavity. The staining color of the new cartilage tissue is uniform and similar to that of the normal tissue, with a good transition between cartilage and the subchondral bone and no significant cartilage and subchondral bone invasion. The bone tissue within the subchondral bone is repaired appropriately, with a moderate amount of bone trabeculae. The volume and shape of the bone trabeculae are most similar to normal tissue. There is good integration between the new tissue and the original tissue. The HE results show that the cartilage and subchondral bone of the defect area injected with the double-layer scaffold is well repaired, and the new tissue is tightly integrated with the surrounding tissue, forming a transparent cartilage most similar to the normal tissue. Injecting only the cartilage layer of the material may achieve the corresponding effect but tends to overgrow and is of little help in repairing the other layer. The articular cartilage and

subchondral bone are tightly integrated, so achieving good results with a single layer is difficult.

Fig. 8 shows the results of the HE staining of the articular cartilage and cartilage tissue at weeks 4 and 8 after decalcification. The staining of safranine O-fast green allows better visual distinction between the articular cartilage and subchondral bone layers. At the defect site (the 2nd column), where only the osteogenic layer scaffold was injected, the subchondral bone is well repaired, with a more uniform distribution of trabeculae. However, there is excessive growth of the subchondral bone into the articular cartilage. It is observed that the new cartilage tissue is fragile, much smaller than normal tissue, with a significant difference in color from the normal tissue. This indicates that the injection of the osteogenic layer material only tends to proliferate the subchondral bone and hardly effectively contributes to articular cartilage regeneration. At the defect site where only the cartilage layer material was injected (the 3rd column), the thickness of the new cartilage is already
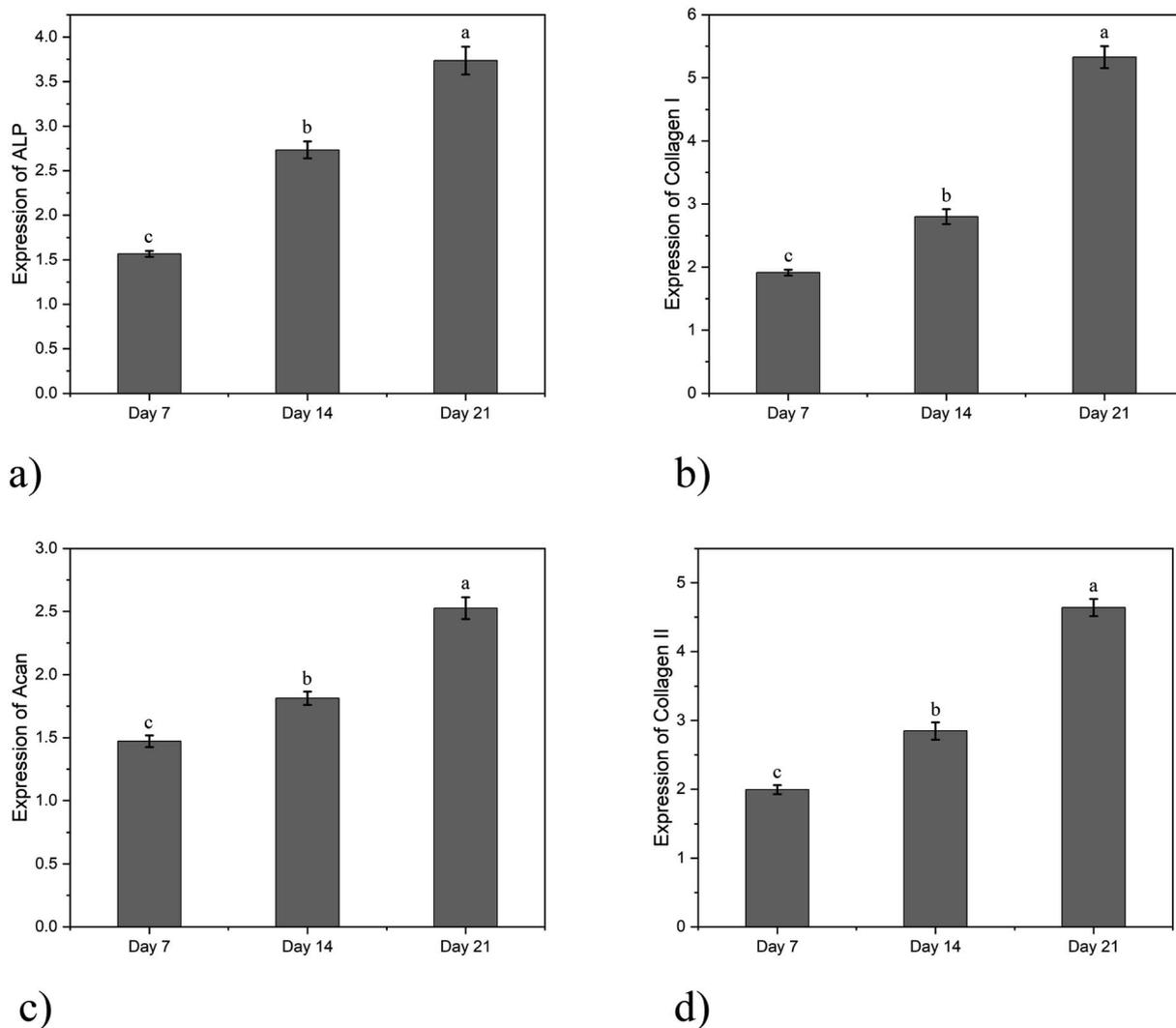
Fig. 5 Gene expression levels of cells in different hydrogels: (a) ALP; (b) collagen I; (c) Acan; (d) collagen II.
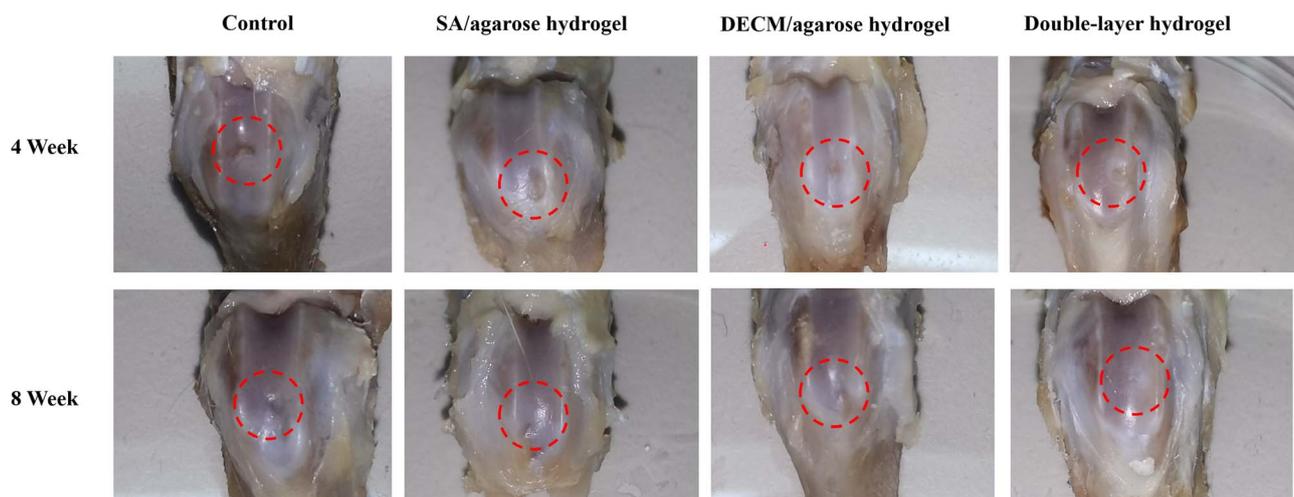

Fig. 6 The appearance of articular cartilage injury samples with different hydrogels at week 4 and week 8.
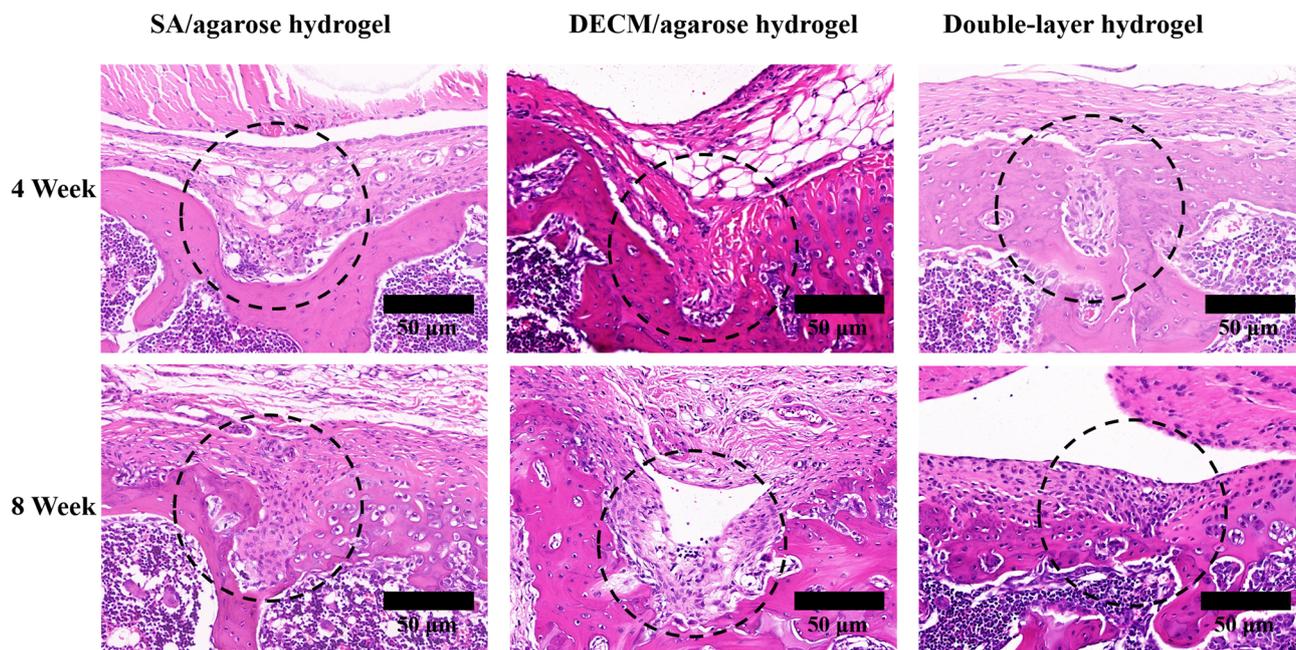
Fig. 7 HE staining images of the samples at different conditions.

greater than the normal tissue at 4 weeks. A large number of chondrocytes are distributed within the new cartilage tissue. However, unclear demarcation also appears between the new cartilage and the subchondral bone, and the new cartilage grows into the subchondral bone. In contrast, the subchondral bone is poorly repaired, with uneven distribution of bone trabeculae and large gaps, indicating that the sole injection of the cartilage layer material only leads to cartilage proliferation and does not significantly contribute to the regeneration of the

subchondral bone. The new cartilage produced in the repair process differs from the hyaline cartilage in the normal articular cartilage tissue. Although there is still some difference in the thickness of the new cartilage layer between the repaired tissue and the normal tissue after 4 weeks, the morphology of the new cartilage is the closest to that of the normal tissue, with a smooth surface and a clear demarcation line between the new cartilage and the subchondral bone, without mutual ingrowth. The bone trabeculae are evenly distributed and regular. After 8
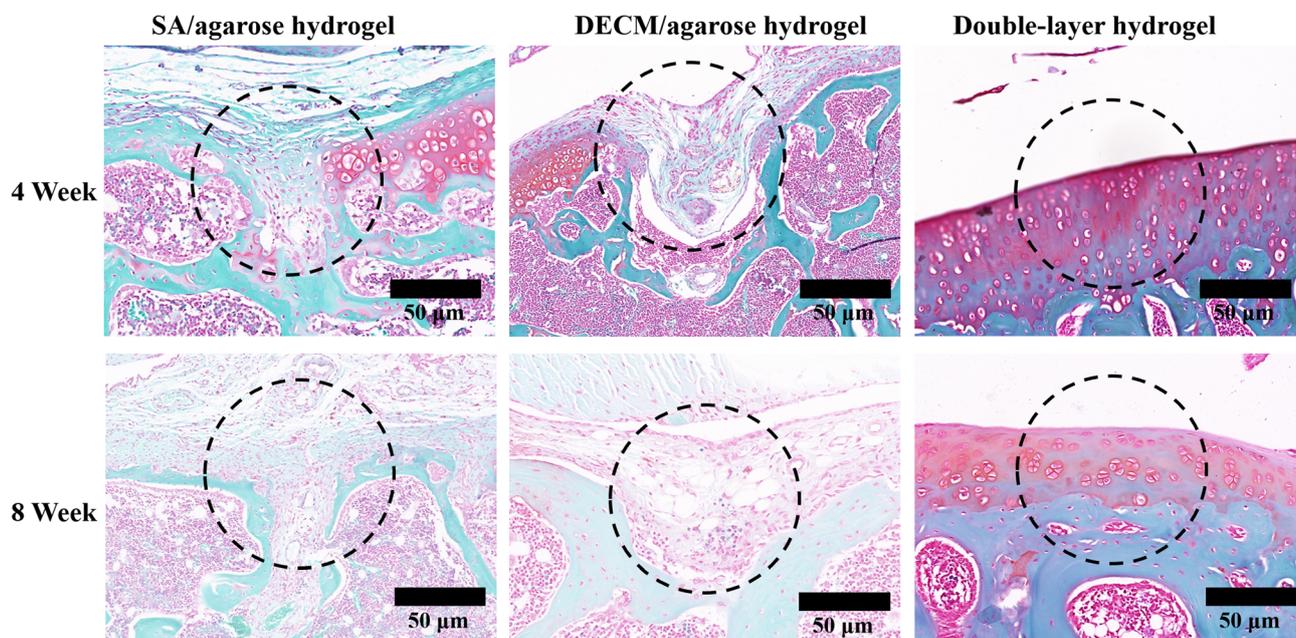

Fig. 8 Safranine O-fast green staining images of the samples at different conditions.

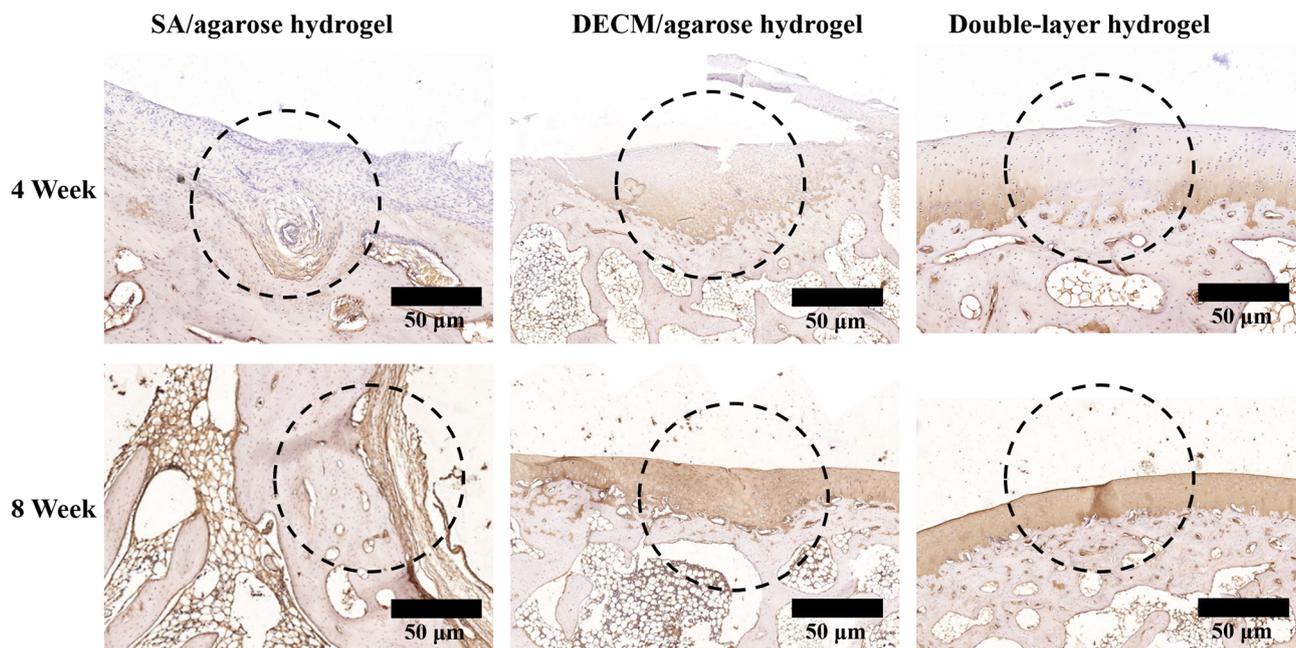| SA/agarose hydrogel | DECM/agarose hydrogel | Double-layer hydrogel |

Fig. 9 Type II collagen IHC staining images of the samples at different conditions.

weeks of repair, the thickness of the new cartilage tissue is very close to the normal cartilage tissue, while their structures and morphologies are very similar, with good regeneration of the subchondral bone. Therefore, the results obtained from the red solid green stain's staining are consistent with the HE staining results. Both datasets indicate that the injection of the double-layered scaffold promotes the regeneration of articular cartilage and subchondral bone. The new cartilage tissue is most similar to the normal articular cartilage staining. In contrast, the sole injection of the single-layer material leads to excessive regeneration and does not contribute significantly to the repair of the other layer. Both approaches exhibit difficulties in producing new hyaline cartilage. The results are similar to those of normal cartilage.

Collagen II immunohistochemical staining of articular cartilage and subchondral bone was performed at 4 and 8 weeks postoperatively, and the results are shown in Fig. 9. More positive collagen II results are observed at the defect site injected with the osteogenic layer scaffold. However, the thickness is low and unevenly distributed, and the surface smoothness is lacking, indicating that although the osteogenic layer material could play a role in articular cartilage regeneration, it does not lead to the complete repair of articular cartilage. As shown in the group injected with the cartilage layer scaffold material, the positive results of collagen II immunohistochemical staining are obvious. The thickness of the cartilage layer even slightly exceeds the thickness of the cartilage layer in normal joints. However, there are significant morphological differences between the new and normal cartilage. Regarding the staining results, the new cartilage in the defect area injected only with the cartilage layer scaffold exhibits more yellow staining results, showing significant differences between the normal tissue and the new cartilage. In contrast, the new

articular cartilage in the defect area injected with the double-layered scaffold material is comparable to the normal tissue in thickness, structure, and staining results. This indicates that using the double-layer scaffold in articular cartilage and sub-chondral bone defects can effectively promote articular cartilage regeneration, and the new cartilage's structure is most similar to the normal cartilage. From the results of animal experiments, the bioactive double-layer injectable hydrogel scaffold can repair the articular cartilage and subchondral bone defects well. The new tissue is similar to the normal tissue and integrates well with the surrounding tissue, which can repair the hyaline cartilage to a certain extent. In contrast, the single-layer hydrogel scaffold can be useful for articular cartilage or subchondral bone defects after injection into the defect site. After injection in the defect area, the single-layer hydrogel scaffold can repair the corresponding articular cartilage or subchondral bone. However, it does not help repair the other tissue layer. Such a sole injection of the single-layer hydrogel scaffold can easily lead to excessive repair of the corresponding tissue and invasion of the other tissue layer.

4 Conclusion

A double-layer injectable bioactive hydrogel scaffold was designed and fabricated to repair articular cartilage and subchondral bone defects with the dECM/agarose hydrogel carrying chondrocytes and bone marrow MSCs and with SA/agarose hydrogel carrying bone marrow MSCs for the repair of subchondral bone, respectively. The regeneration of articular cartilage cannot be achieved without a suitable mechanical environment provided by the subchondral bone. Therefore, articular cartilage and subchondral bone should be repaired as a whole system. We designed a bioactive injectable double-layer

hydrogel scaffold which is a temperature-sensitive pre-gel solution capable of gelation near 37 °C. The scaffold prepared from the hydrogel has good hydrophilicity and adequate porosity, and its mechanical strength is suitable to become a scaffold material for osteochondral repair, which can play a substitute role before articular cartilage repair. Meanwhile, seed cells can survive and proliferate and differentiate well in the material. In animal experiments, simultaneous injection of double-layered tissue-engineered scaffolds into the injury site can promote the regeneration of both articular cartilage and subchondral bone, and the morphology of the new cartilage is closer to that of the normal articular hyaline cartilage. At the same time, the transition between the new cartilage and the subchondral bone is clearly demarcated. The bond between the new tissue and the original tissue is tight, and the material is effective for the repair of cartilage and subchondral bone defects.

Ethical statement

All animal procedures were performed in accordance with the Guidelines for Care and Use of Laboratory Animals of Guangdong Provincial People's Hospital and approved by the Animal Ethics Committee of Guangdong Provincial People's Hospital.

Conflicts of interest

The authors declare no competing financial interest.

Acknowledgements

References

1 B. J. Cole, M. L. Redondo and E. J. Cotter, *Cartilage*, 2021, **12**, 139–145.

2 B. J. Huang, J. C. Hu and K. A. Athanasiou, *Biomaterials*, 2016, **98**, 1–22.

3 Q. Zhang, Y. Hu, X. Long, L. Hu, Y. Wu, J. Wu, X. Shi, R. Xie, Y. Bi, F. Yu, P. Li and Y. Yang, *Front. Bioeng. Biotechnol.*, 2022, **10**, 908082.

4 A. Goldberg, K. Mitchell, J. Soans, L. Kim and R. Zaidi, *J. Orthop. Surg. Res.*, 2017, **12**, 39.

5 M. P. Murphy, L. S. Koepke, M. T. Lopez, X. Tong, T. H. Ambrosi, G. S. Gulati, O. Marecic, Y. Wang, R. C. Ransom, M. Y. Hoover, H. Steininger, L. Zhao, M. P. Walkiewicz, N. Quarto, B. Levi, D. C. Wan, I. L. Weissman, S. B. Goodman, F. Yang, M. T. Longaker and C. K. F. Chan, *Nat. Med.*, 2020, **26**, 1583–1592.

6 H. L. Stewart and C. E. Kawcak, *Front. Vet. Sci.*, 2018, **5**, 178.

7 J. Jiang, A. Tang, G. A. Ateshian, X. E. Guo, C. T. Hung and H. H. Lu, *Ann. Biomed. Eng.*, 2010, **38**, 2183–2196.

8 W. Wei and H. Dai, *Bioact. Mater.*, 2021, **6**, 4830–4855.

9 J. Huang, Q. Liu, J. Xia, X. Chen, J. Xiong, L. Yang and Y. Liang, *J. Transl. Med.*, 2022, **20**, 515.

10 C. E. Kilmer, T. Walimbe, A. Panitch and J. C. Liu, *ACS Biomater. Sci. Eng.*, 2022, **8**, 1247–1257.

11 E. Lee, I. E. Epanomeritakis, V. Lu and W. Khan, *Int. J. Mater. Sci.*, 2023, **24**, 3227.

12 K. To, B. Zhang, K. Romain, C. Mak and W. Khan, *Front. Bioeng. Biotechnol.*, 2019, **7**, 314.

13 S. S. H. Tan, C. K. E. Tjio, J. R. Y. Wong, K. L. Wong, J. R. J. Chew, J. H. P. Hui and W. S. Toh, *Tissue Eng., Part B*, 2021, **27**, 1–13.

14 N. Bakhtiary, C. Liu and F. Ghorbani, *Gels*, 2021, **7**, 274.

15 X. Zhao, X. Chen, H. Yuk, S. Lin, X. Liu and G. Parada, *Chem. Rev.*, 2021, **121**, 4309–4372.

16 R. M. Natoli and K. A. Athanasiou, *Biorheology*, 2009, **46**, 451–485.

17 L. Zhou, V. O. Gjvm, J. Malda, M. J. Stoddart, Y. Lai, R. G. Richards, K. Ki-wai Ho and L. Qin, *Adv. Healthcare Mater.*, 2020, **9**, 2001008.

18 E. M. Darling and K. A. Athanasiou, *J. Orthop. Res.*, 2005, **23**, 425–432.

19 V. V. Meretoja, R. L. Dahlin, F. K. Kasper and A. G. Mikos, *Biomaterials*, 2012, **33**, 6362–6369.

20 M. F. Pittenger, A. M. Mackay, S. C. Beck, R. K. Jaiswal, R. Douglas, J. D. Mosca, M. A. Moorman, D. W. Simonetti, S. Craig and D. R. Marshak, *Science*, 1999, **284**, 143–147.

21 S. Zhang, S. J. Chuah, R. C. Lai, J. H. P. Hui, S. K. Lim and W. S. Toh, *Biomaterials*, 2018, **156**, 16–27.

22 Y. Chen, X. Ouyang, Y. Wu, S. Guo, Y. Xie and G. Wang, *CSCR*, 2020, **15**, 54–60.

23 P. Apelgren, E. Karabulut, M. Amoroso, A. Mantas, H. Martínez Ávila, L. Kölby, T. Kondo, G. Toriz and P. Gatenholm, *ACS Biomater. Sci. Eng.*, 2019, **5**, 2482–2490.

24 Z. Tang, Y. Lu, S. Zhang, J. Wang, Q. Wang, Y. Xiao and X. Zhang, *J. Mater. Chem. B*, 2021, **9**, 9989–10002.

25 S. Zhang, S. J. Chuah, R. C. Lai, J. H. P. Hui, S. K. Lim and W. S. Toh, *Biomaterials*, 2018, **156**, 16–27.

26 X. Yu, Z. Deng, H. Li, Y. Ma, X. Ma and Q. Zheng, *RSC Adv.*, 2022, **12**, 28254–28263.

27 N. Huebsch, P. R. Arany, A. S. Mao, D. Shvartsman, O. A. Ali, S. A. Bencherif, J. Rivera-Feliciano and D. J. Mooney, *Nat. Mater.*, 2010, **9**, 518–526.

28 S. H. Oh, D. B. An, T. H. Kim and J. H. Lee, *Acta Biomater.*, 2016, **35**, 23–31.